Journal of Applied Mechanics and Technical Physics, Vol. 51, No. 3, pp. 308–316, 2010

DEVELOPMENT OF THE RICHTMYER–MESHKOV INSTABILITY DURING INTERACTION OF THE DIFFUSION MIXING LAYER OF TWO GASES WITH TRANSIENT AND REFLECTED SHOCK WAVES

G. A. Ruev,[1] A. V. Fedorov[2], and V. M. Fomin[2]

UDC 532.517.4:533.6.011.8

The evolution of the initially disturbed mixing layer of two gases of different densities under the action of an incident shock wave, shock waves reflected from the end face, compression and expansion waves is studied in a two-dimensional unsteady approximation on the basis of the previously formulated mathematical model of mechanics of a two-velocity two-temperature mixture of gases. Problems of wave interaction with a sinusoidally disturbed diffusion layer are solved numerically. It is shown that the calculated width of the mixing region is in good agreement with experimental data.

Key words: *shock wave, mixing layer, Richtmyer–Meshkov instability, two-velocity two-temperature gas dynamics of mixtures.*

Introduction. The mixing layer is usually considered as a surface of density discontinuity, i.e., as a contact discontinuity. The shock wave interaction with the disturbed contact discontinuity generates the Richtmyer–Meshkov instability [1, 2]. A region of turbulent mixing separating the compressed gas flows is formed at the final stage in the region of the initial contact discontinuity.

In numerous publications dealing with numerical modeling of the Richtmyer–Meshkov instability evolution (see, e.g., [3–5]) with the use of the Euler equations, the effect of the processes of mutual penetration of the gases was ignored. It is also known that replacement of a stepwise density profile on the contact discontinuity by a continuous distribution in a certain finite-width layer can reduce the growth rate of disturbances at the initial stage of the Richtmyer–Meshkov instability evolution. This fact was noted, for instance, in theoretical works [6, 7] where the increase in the disturbance amplitude was studied and also in experimental works [8–10]. Therefore, it seems of interest to study this problem with the use of equations for a two-velocity two-temperature mixture of gases, where each species has its own velocity and temperature. This approach provides a description of both the processes of mutual penetration of the gases and the interaction of the mixing layer with the shock wave. The necessity of using models of multispecies mixtures for the description of contact boundary destruction and mixing region formation was noted in [11]. Youngs [5] constructed a semi-empirical model of turbulent mixing of a multispecies medium with allowance for the velocity of each species. This model implied that turbulent mixing emerged instantly. Interaction of the mixing layer with an incident shock wave [12] and with a compression wave [13] was studied previously. The processes of the Richtmyer–Meshkov instability with allowance for multiple interactions of the mixing layer with reflected waves are studied below with the use of equations of two-velocity two-temperature gas dynamics of the mixtures.

Formulation of the Problem. We study the evolution of the transitional layer separating two pure gases of different densities within the framework of the model of a two-dimensional unsteady flow of a two-velocity two-temperature mixture under the action of a shock wave on this layer (Fig. 1). A steady shock wave propagates from

[1]Novosibirsk State University of Architecture and Civil Engineering, Novosibirsk 630008; ruev@sibstrin.ru. [2]Khristianovich Institute of Theoretical and Applied Mechanics, Siberian Division, Russian Academy of Sciences, Novosibirsk 630090; fedorov@itam.nsc.ru. Translated from Prikladnaya Mekhanika i Tekhnicheskaya Fizika, Vol. 51, No. 3, pp. 14–23, May–June, 2010. Original article submitted May 6, 2009; revision submitted June 17, 2009.

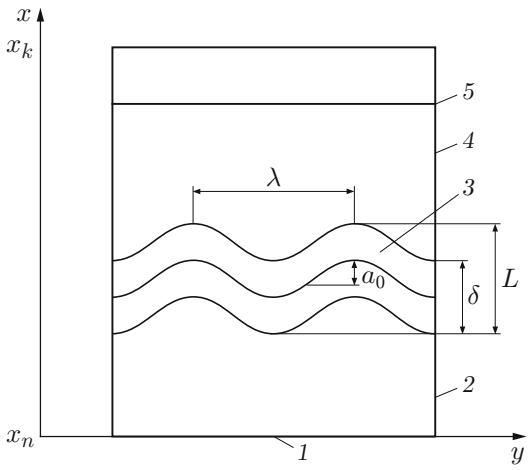

Fig. 1. Schematic of the problem of the evolution of disturbances on the interface of two media: 1) solid wall; 2) gas No. 1; 3) mixing layer; 4) gas No. 2; 5) shock wave.

gas No. 2 to gas No. 1. At the time $t = 0$, the shock wave arrives on the layer boundary. The equation of the mixing layer centerline has the form $x_0(y) = a_0(1 - \cos(\theta y))$, where a_0 is the disturbance amplitude, $\theta = 2\pi/\lambda$ is the wavenumber, and λ is the disturbance wavelength. The total width of the mixing layer is denoted by L, and the initial width of the diffusion layer is denoted by δ. In what follows, the mixing layer takes part in multiple interactions with the waves reflected from the wall $x = x_n$.

The parameters of the mixture in the layer are described by the equations of two-velocity two-temperature gas dynamics of the mixtures [14]:

$$\frac{\partial \boldsymbol{U}_i}{\partial t} + \frac{\partial \boldsymbol{F}_i^{(1)}}{\partial x} + \frac{\partial \boldsymbol{F}_i^{(2)}}{\partial y} = \boldsymbol{W}_i,$$

$$\boldsymbol{U}_i = \begin{bmatrix} \rho_i, \\ \rho_i u_i, \\ \rho_i v_i, \\ E_i \end{bmatrix}, \qquad \boldsymbol{F}_i^{(1)} = \begin{bmatrix} \rho_i u_i, \\ \rho_i u_i^2 + p_i, \\ \rho_i u_i v_i, \\ u_i E_i + p_i u_i \end{bmatrix}, \qquad \boldsymbol{F}_i^{(2)} = \begin{bmatrix} \rho_i v_i, \\ \rho_i v_i u_i, \\ \rho_i v_i^2 + p_i, \\ v_i E_i + p_i v_i \end{bmatrix}, \tag{1}$$

$$\boldsymbol{W}_i = \begin{bmatrix} 0, \\ K(u_j - u_i), \\ K(v_j - v_i), \\ K u_i(u_j - u_i) + K v_i(v_j - v_i) + \beta_i K((u_j - u_i)^2 + (v_j - v_i)^2) + q(T_j - T_i) \end{bmatrix},$$

$$p_i = k n_i T_i, \quad E_i = \rho_i\Big(e_i + \frac{u_i^2 + v_i^2}{2}\Big), \quad e_i = \frac{k T_i}{m_i(\gamma_i - 1)}, \quad \rho_i = m_i n_i, \quad i, j = 1, 2 \ (i \neq j).$$

Here, ρ_i is the density, u_i and v_i are the velocity components, e_i is the internal energy, p_i is the pressure, T_i is the temperature, m_i is the molecule mass, n_i is the number density of molecules of the ith kind, x and y are the Cartesian coordinates, t is the time, k is the Boltzmann constant, $K = 16\rho_1\rho_2\Omega_{12}^{(1,1)}/(3(m_1 + m_2))$, $\Omega_{12}^{(1,1)}$ is the collision integral, $\beta_i = m_i T_i/(m_1 T_1 + m_2 T_2)$, $q = 3m_1 K/(m_1 + m_2)$, E_i is the total energy of the ith species, and γ_i is the ratio of specific heats. The relation for the interaction potential of hard spheres is written in the form

$$K = \frac{16}{3}\,\frac{\rho_1\rho_2}{m_1 m_2}\sqrt{\frac{k\pi}{2}}\sqrt{\frac{T_1}{m_1} + \frac{T_2}{m_2}}\,\sigma_{12}, \qquad \sigma_{12} = \frac{\sigma_1 + \sigma_2}{2}$$

(σ_i is the diameter of the molecules of the ith gas).

The relation $K = x_1 x_2 p/D$ (D is the diffusion coefficient) is valid for a one-temperature medium.

At small (or zero) values of the concentration of the jth gas, the Euler equations for the pure ith gas are used, and the second gas parameters are determined from the relations

$$\frac{\partial n_j}{\partial t} + \frac{\partial n_j u_j}{\partial x} + \frac{\partial n_j v_j}{\partial y} = 0, \qquad u_j = u_i, \qquad v_j = v_i, \qquad T_j = T_i.$$

The transition from one system of equations to the other is performed under the condition that the maximum value between the molar and mass fractions of the ith gas does not exceed 0.1%: $\max(x_i, \alpha_i) \leqslant 0.1\%$, $x_i = n_i/(n_1 + n_2)$, and $\alpha_i = \rho_i/(\rho_1 + \rho_2)$.

Formation of the Initial Mixing Region. An asymptotic solution of the problem of formation of the initial diffusion layer was obtained in [15] in the one-dimensional approximation. Assuming that the distribution of parameters in each y section remains one-dimensional in the presence of disturbances, we obtain the relation for the molar fraction in the layer [15]

$$x_1 = (1 - \Phi(\eta))/2, \tag{2}$$

satisfying the initial distribution of the molar fraction: $x_1 = 1$ at $x < x_0(y)$ and $x_1 = 0$ at $x > x_0(y)$. In Eq. (2), we have

$$\Phi(\eta) = \frac{2}{\sqrt{\pi}} \int\limits_0^\eta \mathrm{e}^{-\omega^2}\, d\omega, \qquad \eta = \frac{x - x_0(y)}{2\sqrt{Dt}}, \qquad D = \frac{x_1 x_2 p}{K}.$$

Calculation Method. The method of vector flux splitting [16] is used as the calculation method for spatial approximation of system (1). For the solution to remain monotonic in the regions of high gradients, the order of approximation is reduced with the minmod limiter used in constructing total variation diminishing (TVD) schemes [17]. The implicit approximation of the right sides of system (1) proposed in [14] is used, which does not require additional restrictions on the time step imposed by the Courant condition. The difference scheme was described in more detail in [13].

The calculations were performed in a rectangular domain $[x_n, x_k; 0, \lambda/2]$. The condition of zero derivatives was imposed on the upper boundary, the lower boundary was a solid wall, and the conditions of symmetry were set on the side boundaries. To eliminate the effects of reflection on the boundary $x = x_k$, we introduced an additional buffer zone in which the x step of the discretized domain was increased with a certain factor (from 1.01 to 1.05). The length of this domain was 100–500 steps. The concentration distribution at the initial time was described by Eq. (2). The remaining parameters ahead of the shock-wave front were defined in the form $u_i = v_i = 0$, $T_i = T_0 = 300$ K, $p = p_0 = 10^5$ Pa, $n = n_0 = p_0/(kT_0)$, and $n_i = x_i n_0$. At the initial time, the shock wave was located in the x cross section (at the layer boundary) where the maximum concentration of gas No. 1 (molar fraction if gas No. 1 is light and mass fraction if gas No. 1 is heavy) is 0.1%. The parameters behind the shock-wave front were found from the Rankine–Hugoniot equations for gas No. 2.

One-Dimensional Study of the Shock-Wave Incidence onto the Mixing Layer with Allowance for Reflection from the Wall. Let us consider the shock-wave interaction with the mixing layer in two cases: when the wave is incident onto the layer when it moves from the light to the heavy gas and vice versa.

Figure 2a shows the pressure on the wall and in the middle of the mixing layer as a function of time in the case of the shock wave with the Mach number M = 1.32 passing from the light gas (air) to the heavy gas (SF_6) (the initial width of the layer before its interaction with the shock wave was 15 mm, and the distance between the mixing layer centerline and the end face at the initial time was 10 cm).

Let us consider the wave pattern of the flow. After interaction with the mixing layer at the time $t = 0.53$ msec, the shock wave reaches the end face of the channel. At the time $t = 0.75$ msec, the shock wave reflected from the wall interacts with the mixing layer. This interaction generates a reflected expansion wave moving over the gas SF_6 and a transient shock wave propagating in air. At $t = 0.87$ msec, the expansion wave reaches the wall and is reflected from it. The reflected expansion wave reaches the mixing layer at the time $t = 1.08$ msec. As a result of this interaction, a compression wave propagates from the mixing layer toward the end face of the channel and reaches the wall at the time $t = 1.3$ msec. The compression wave reflected from the end face moves toward the mixing layer. The process is repeated and is characterized by alternation of reflected expansion and compression waves moving between the end face of the channel and the mixing layer with a decreasing amplitude. Figure 2a also shows the dependence of the mixing layer centerline position versus time. As a result of pulsed acceleration under the action of the incident shock wave, the mixing layer moves with a constant velocity toward the end face of the

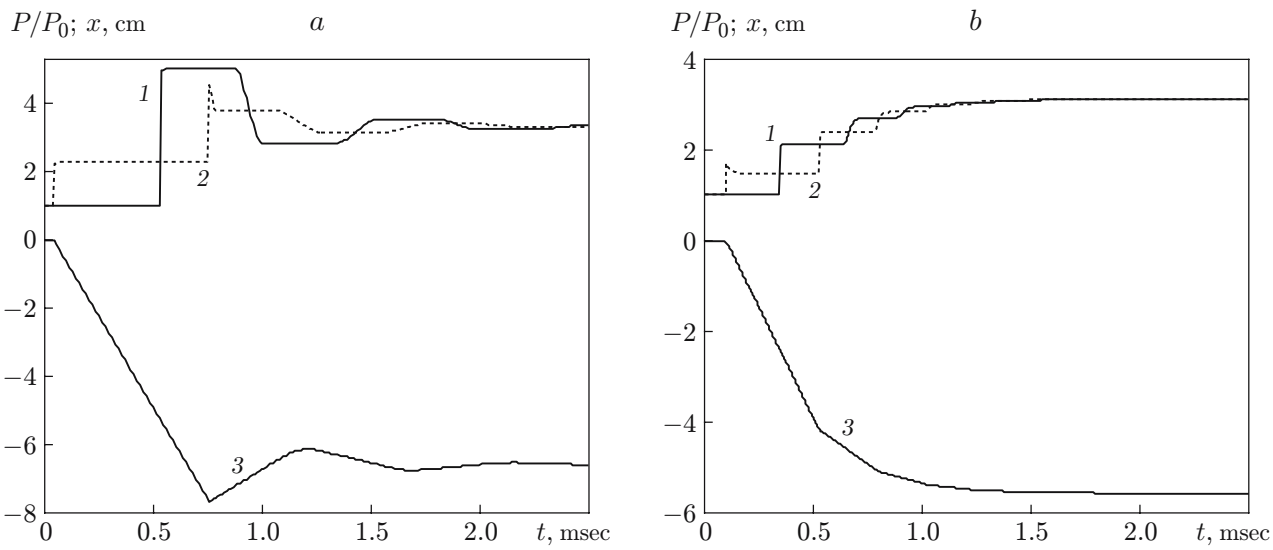

Fig. 2. Pressure of the mixture on the walls (1) and in the middle of the layer (2), and also position of the mixing layer centerline (3) versus time: (a) the shock wave moves from the light gas (air) to the heavy gas (SF_6); (b) the shock wave moves from the heavy gas (SF_6) to the light gas (air).

channel, then it starts moving in the direction away from the end face under the action of the reflected shock wave, and then again moves toward the end face of the channel owing to the formation of the expansion wave reflected from the mixing layer. After small oscillations, the layer then returns to the equilibrium state. This description of the process of mixing layer interaction with the incident waves and the waves reflected from the end face is consistent with the description given in [18].

Figure 2b shows the time evolution of the pressure on the wall and in the middle of the mixing layer when the shock wave (M = 1.32) moves from the heavy gas (SF_6) to the light gas (air). In this case, after reflection of the incident shock wave from the end face of the channel, there arises a series of reflected compression waves with a decreasing amplitude, which propagate between the end face and the mixing layer. As a result, the layer returns to the equilibrium state. Figure 2b also shows the position of the mixing layer centerline versus time. It is seen that the velocity of the layer first increases as a result of interaction with the incident shock wave and then gradually decreases under the action of the reflected compression waves.

Plane-Case Study of Shock-Wave Incidence onto a Sinusoidally Disturbed Mixing Layer with Allowance for Reflection from the Wall. Let us consider the evolution of disturbances in the mixing layer interacting with the incident shock wave in the case where gas No. 2 is light and gas No. 1 is heavy (see Fig. 1).

Figure 3 shows the isolines of the molar fraction of the heavy gas SF_6 at different time instants after the beginning of interaction with the incident shock wave. We considered the shock wave with the Mach number M = 1.32 passing from air to the gas SF_6 (the diffusion coefficient was $D = 0.097$ cm$^2\cdot$sec^{-1} [18], the ratio of molecular weights was $m_{\text{air}}/m_{SF_6} = 29.04/146.07$, the distance from the mixing layer centerline to the end face of the channel at the initial time was 10 cm, the initial width of the mixing layer was 15 mm, the initial length of the disturbance wave was 6 cm, and the initial disturbance amplitude was 1 mm).

As a result of shock-wave interaction with the mixing layer, the latter becomes compressed; when the shock wave leaves the layer, the disturbance amplitude starts to increase, as was described in [12]. After that, the layer interacts with the shock wave reflected from the end face, which leads to its straightening ($t = 0.9$ msec), and the disturbance phase changes (the reflected wave propagates from the heavy to the light gas). A heavy gas jet with formation of a mushroom-shaped structure and vortices on the jet boundary appears later.

Figure 4 shows the disturbance amplitude as a function of time, which were obtained in the present work and in the experiments [9] for the shock wave with the Mach number M = 1.32 propagating from air to the gas SF_6 (t_1 and t_2 are the times of the first contact of the reflected shock wave with the mixing layer, corresponding to curves 1 and 2). It is seen that the disturbance amplitude drastically increases after interaction of the reflected shock wave with the mixing layer.

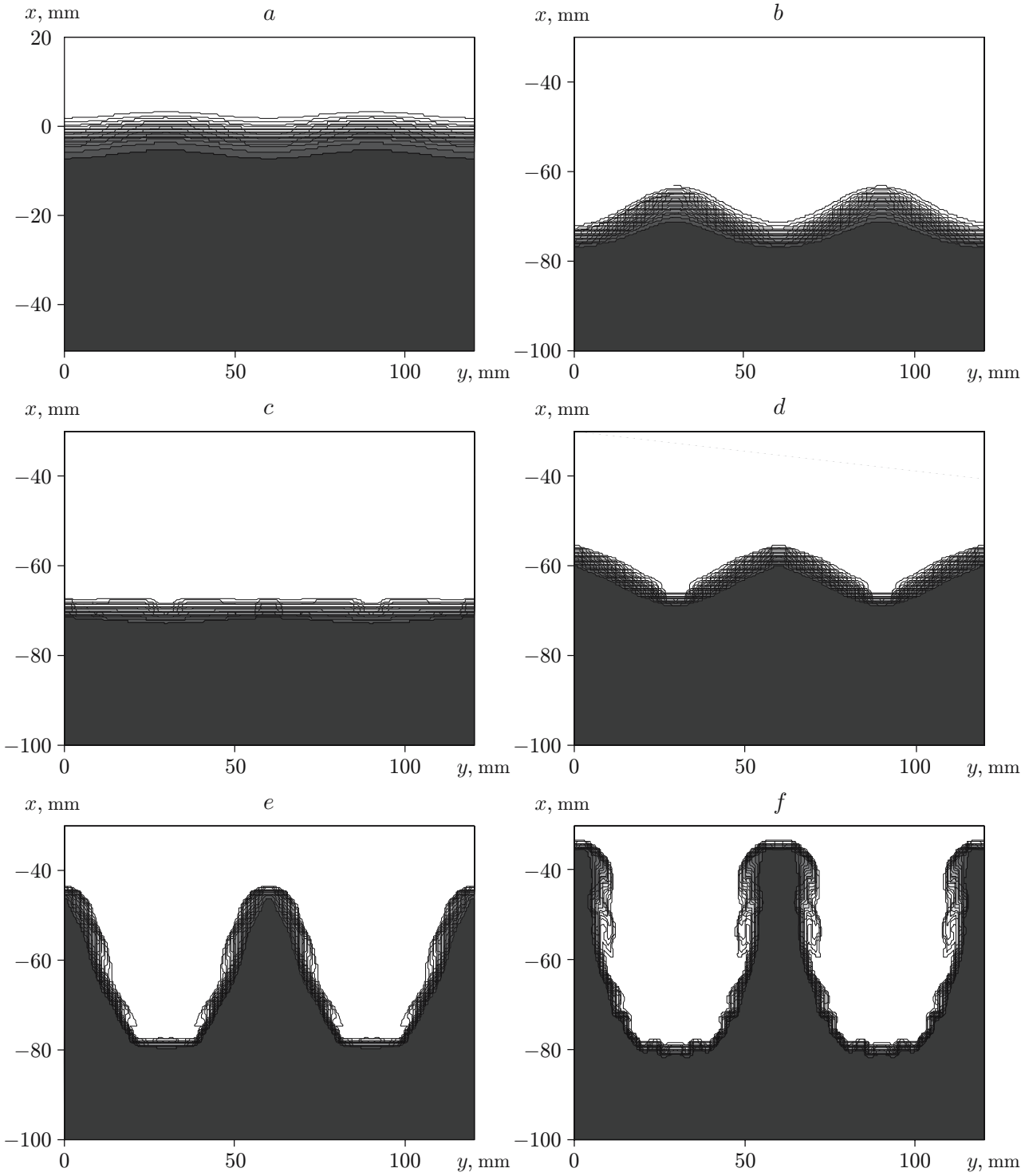

Fig. 3. Isolines of the molar fraction of the gas SF_6 in the case of shock-wave propagation from the light to the heavy gas at different times: $t = 0$ (a), 0.7 (b), 0.9 (c), 1.1 (d), 1.5 (e), and 2.0 msec (f).

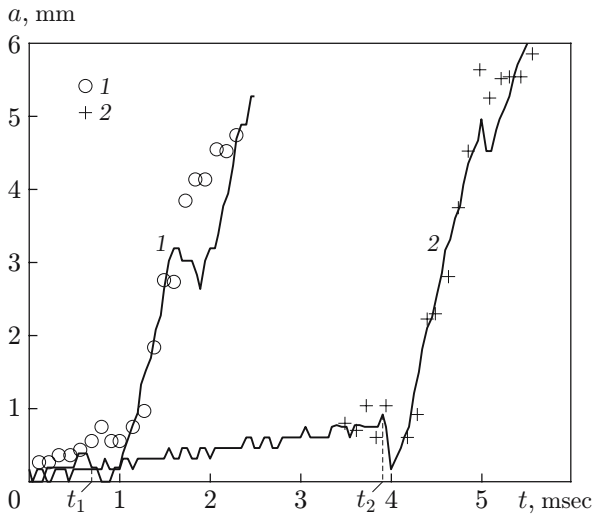

Fig. 4

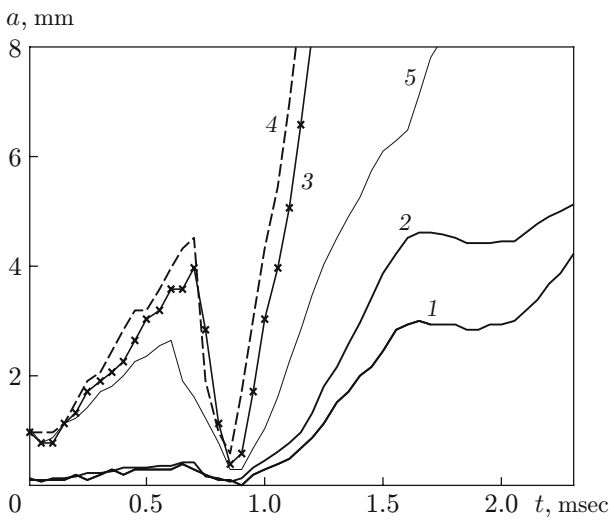

Fig. 5

Fig. 4. Disturbance amplitude versus time for different distances from the mixing layer centerline to the end face of the channel at the initial time instant: 10 (1) and 55 cm (2); the curves and points show the calculated and experimental [9] data.

Fig. 5. Disturbance amplitude versus time for different values of parameters: curves 1–4 refer to the case where the shock wave propagates from air to the gas SF_6 with $a_0 = 0.1$ mm, $\lambda = 6$ cm, and $\delta_0 = 15$ mm (1), $a_0 = 0.1$ mm, $\lambda = 5$ cm, and $\delta_0 = 15$ mm (2), $a_0 = 1$ mm, $\lambda = 6$ cm, and $\delta_0 = 15$ mm (3), and $a_0 = 1$ mm, $\lambda = 6$ cm, and $\delta_0 = 7$ mm (4); curve 5 shows the case where the shock wave propagates from argon to xenon ($a_0 = 1$ mm, $\lambda = 6$ cm, and $\delta_0 = 15$ mm).

Figure 5 shows the disturbance amplitude as a function of time for different values of parameters in the case of the shock wave with the Mach number M = 1.32 propagating from air to the gas SF_6. It is seen that an increase in the disturbance amplitude, a decrease in the disturbance wavelength, and a decrease in the initial width of the layer lead to a more rapid growth of the disturbance amplitude. Figure 5 also shows the calculated increase in the disturbance amplitude for the shock wave propagating from argon to xenon [the ratio of molecular weights is 3.28 (curve 5), whereas the ratio of molecular weights for air and the gas SF_6 is 5.03 (curve 3)]. It is seen that the disturbance amplitude increases with increasing ratio of molecular weights.

Let us consider the evolution of disturbances in the mixing layer with the incident shock wave in the case where gas No. 2 is heavy (SF_6) and gas No. 1 is light (air). The shock wave with the Mach number M = 1.32 propagates from the gas SF_6 to air, the distance from the mixing layer centerline to the end face at the initial time is 10 cm, the initial width of the mixing layer is 15 mm, the initial disturbance wavelength is 6 cm, and the initial disturbance amplitude is 1 mm.

Figure 6 shows the isolines of the molar fraction of the heavy gas SF_6 at different times after the beginning of interaction with the incident shock wave. In this case, the incident shock wave propagates from the heavy to the light gas, and the disturbance phase changes before the reflected shock wave arrives. In what follows, additional actions of the reflected compression waves forms a heavy gas jet with subsequent formation of a mushroom-shaped structure.

Figure 7 shows the time evolution of the disturbance amplitude for different values of parameters in the case of propagation of the shock wave with the Mach number M = 1.32 from the gas SF_6 to air. It is seen that an increase in the disturbance amplitude, a decrease in the disturbance wavelength, a decrease in the initial width of the layer, and an increase in the Mach number lead to a more rapid increase in the disturbance amplitude. The growth of disturbances in the case of shock-wave propagation from the light to the heavy gas is more intense than in the case of shock-wave propagation from the heavy to the light gas. Deceleration of the growth of disturbances at M = 1.5 (curve 5) is caused by the fact that the layer reaches the end face of the channel.

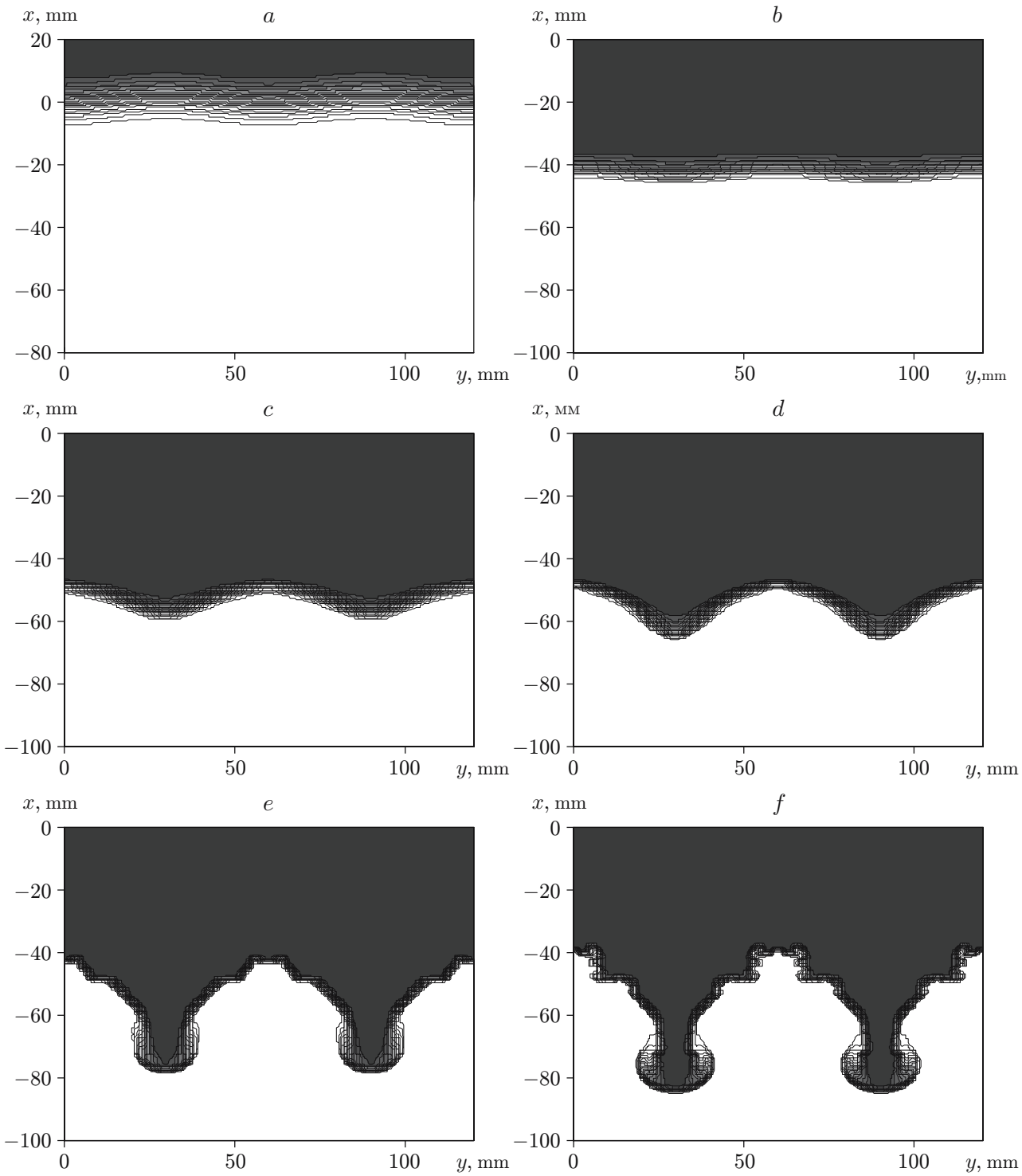

Fig. 6. Isolines of the molar fraction of the gas SF_6 for the shock wave propagating from the heavy to the light gas at $t = 0$ (a), 0.5 (b), 0.9 (c), 1.2 (d), 2 (e), and 2.5 msec (f).

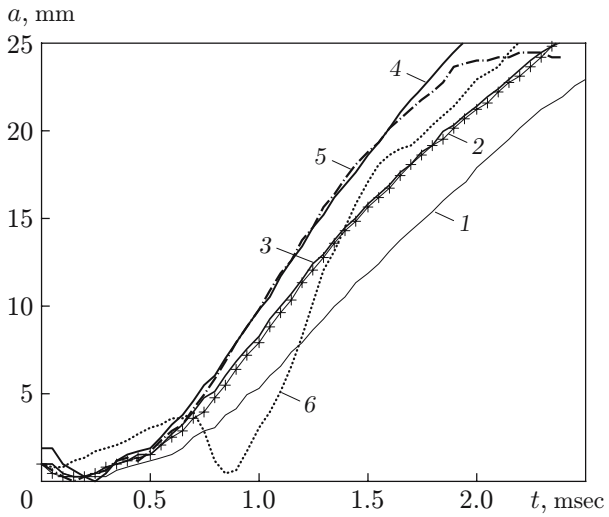

Fig. 7. Disturbance amplitude versus time for different values of parameters: curves 1–5 refer to the case where the shock wave propagates from the gas SF_6 to air with $a_0 = 1$ mm, $\lambda = 6$ cm, $\delta_0 = 15$ mm, and M = 1.32 (1), $a_0 = 1$ mm, $\lambda = 6$ cm, $\delta_0 = 7$ mm, and M = 1.32 (2), $a_0 = 1$ mm, $\lambda = 4$ cm, $\delta_0 = 7$ mm, and M = 1.32 (3), $a_0 = 2$ mm, $\lambda = 6$ cm, $\delta_0 = 15$ mm, and M = 1.32 (4), and $a_0 = 1$ mm, $\lambda = 6$ cm, $\delta_0 = 15$ mm, and M = 1.5 (5); curve 6 refers to the case where the shock wave propagates from air to the gas SF_6 [$a_0 = 1$ mm, $\lambda = 6$ cm, $\delta_0 = 15$ mm, and M = 1.32 (curve 3 in Fig. 5)].

Conclusions. The processes of interaction of shock waves with a sinusoidally disturbed mixing region of two gases with allowance for multiple reflections of the waves from the end face of the channel are described with the use of the mathematical model of a two-velocity two-temperature mixture of gases [12–15].

The analysis of the wave patterns of the flow for the cases with the light and heavy gases near the wall shows that they are substantially different.

The mathematical model is verified through comparisons with the measured disturbance amplitudes in the mixing layer.

This work was supported by the Russian Foundation for Basic Research (Grant No. 06-01-00299), by the project entitled "Dynamics of Processes and Boundaries" of the Siberian Division of the Russian Academy of Sciences, and by the Analytical Departmental Targeted Program entitled "Development of the Scientific Potential of the Higher Education" in 2009 (Project code 2.1.1/4674).

REFERENCES

1. R. D. Richtmyer, "Taylor instability in shock acceleration of compressible fluids," *Comm. Pure Appl. Math.*, **13**, 297–319 (1960).
2. E. E. Meshkov, "Instability on a shock-wave accelerated interface of two gases," *Izv. Akad. Nauk SSSR, Mekh. Zhidk. Gaza*, No. 5, 151–157 (1969).
3. O. M. Belotserkovskii, V. V. Demchenko, and A. M. Oparin, "Consecutive transition to turbulence in the Richtmyer–Meshkov instability," *Dokl. Ross. Akad. Nauk*, **334**, No. 5, 581–583 (1994).
4. I. G. Lebo, V. V. Nikishin, V. B. Rozanov, and V. F. Tishkin, "On the effect of boundary conditions on the instability growth at a contact surface in passage of a shock wave," *Bull. Lebedev Phys. Inst.*, No. 1, 40–47 (1997).
5. D. L. Youngs, "Numerical simulation of mixing by Rayleigh–Taylor and Richtmyer–Meshkov instabilities," *Laser Particle Beams*, **12**, No. 4, 725–750 (1994).
6. S. Chandrasekhar, *Hydrodynamics and Hydromagnetic Stability*, Oxford Univ., Oxford (1961), pp. 428–436.
7. B. B. Chakraborty, "Rayleigh–Taylor instability of heavy fluid," *Phys. Fluids*, **18**, No. 8, 1066, 1067 (1975).

8. R. E. Duff, F. H. Harlow, and C. W. Hirt, "Effects of diffusion on interface instability between gases," *Phys. Fluids*, **5**, No. 4, 417–425 (1962).
9. M. Brouillette and B. Sturtevant, "Experiments on the Richtmyer–Meshkov instability: Single-scale perturbations on a continuous interface," *J. Fluid Mech.*, **263**, 271–292 (1994).
10. S. G. Zaitsev, S. N. Titov, and E. I. Chebotareva, "Evolution of the transitional layer separating gases of different densities with a shock wave passing through the layer," *Izv. Ross. Akad. Nauk, Mekh. Zhidk. Gaza*, No. 2, 18–26 (1994).
11. V. F. Kuropatenko, "Unsteady flow of multispecies media," in: *Numerical Methods of Solving Filtration Problems. Dynamics of Multiphase Media* (collected scientific papers) [in Russian], Inst. Theor. Appl. Mech., Sib. Div., Acad. of Sci. of the USSR (1989), pp. 128–155.
12. G. A. Ruev, A. V. Fedorov, and V. M. Fomin, "Development of the Richtmyer–Meshkov instability upon interaction of a diffusion mixing layer of two gases with shock waves," *J. Appl. Mech. Tech. Phys.*, **46**, No. 3, 307–314 (2005).
13. G. A. Ruev, A. V. Fedorov, and V. M. Fomin, "Development of the Rayleigh–Taylor instability due to interaction of a diffusion mixing layer of two gases with compression waves," *Shock Waves*, **16**, No. 1, 65–74 (2006).
14. S. P. Kiselev, G. A. Ruev, A. P. Trunev, et al., *Shock-Wave Processes in Two-Component and Two-Phase Media* [in Russian], Nauka, Novosibirsk (1992).
15. G. A. Ruev, A. V. Fedorov, and V. M. Fomin, "Evolution of the diffusion mixing layer of two gases upon interaction with shock waves," *J. Appl. Mech. Tech. Phys.*, **45**, No. 3, 328–334 (2004).
16. W. K. Anderson, J. L. Thomas, and B. van Leer, "Comparison of finite volume flux vector splittings for the Euler equations," *AIAA J.*, **24**, No. 9, 1453–1460 (1986).
17. S. R. Chakravarthy and S. Osher, "A new class of high accuracy TVD schemes for hyperbolic conservation laws," AIAA Paper No. 85-0363 (1985).
18. M. Brouillette and B. Sturtevant, "Growth induced by multiple shock waves normally incident on plane gaseous interfaces," *Physica D*, **37**, 248–263 (1989).